Effect of Miscibility and Percolation on Electron Transport in Amorphous Poly(3-Hexylthiophene)/Phenyl-C_{61}-Butyric Acid Methyl Ester Blends

Kiarash Vakhshouri, Derek R. Kozub, Chenchen Wang, Alberto Salleo, and Enrique D. Gomez

Phys. Rev. Lett. **108**, 026601 — Published 11 January 2012

DOI: 10.1103/PhysRevLett.108.026601

Effect of Miscibility and Percolation on Electron Transport in Amorphous Poly(3-Hexylthiophene)/Phenyl-C_{61}-Butyric Acid Methyl Ester Blends

*Kiarash Vakhshouri,[†] Derek R. Kozub,[†] Chenchen Wang,[‡] Alberto Salleo[‡] and Enrique D. Gomez[†,§,]**

[†] Department of Chemical Engineering, The Pennsylvania State University, University Park, Pennsylvania 16802

[‡] Materials Science and Engineering, Stanford University, Stanford, California 94305

[§] Materials Research Institute, The Pennsylvania State University, University Park, Pennsylvania 16802

*Address correspondence to: edg12@psu.edu

ABSTRACT:

Recent evidence has demonstrated that amorphous mixed phases are ubiquitous within mesostructured polythiophene/fullerene mixtures. Nevertheless, the role of mixing within nanophases on charge transport of organic semiconductor mixtures is not fully understood. To this end, we have examined the electron mobility in amorphous blends of poly(3-hexylthiophene) and phenyl-C_{61}-butyric acid methyl ester. Our studies reveal that the miscibility of the components strongly affects electron transport within blends. Immiscibility promotes efficient electron transport by promoting percolating pathways within organic semiconductor mixtures. As a consequence, partial miscibility may be important for efficient charge transport in polythiophene/fullerene mixtures and organic solar cell performance.

The generation of unique properties through mixing of organic semiconductors has enabled improved performance and novel functionalities in organic electronic devices [1-3]. In organic light emitting diodes, isolated phases of a second material within the active layer can act as recombination centers, enhancing the quantum efficiency [1]. Mixing of flexible polymer semiconductors with high-mobility small organic molecules can yield high-performance flexible transistors [2]. Solution-processed organic solar cells rely on the self-assembly of polymer/fullerene donor/acceptor mixtures to create the morphology necessary for efficient photocurrent generation [4, 5]. Despite the importance of creating organic semiconductor mixtures and the tremendous recent advances in the performance of the aforementioned devices, it remains a challenge to fully describe the optoelectronic properties of heterogeneous organic semiconductors.

The difficulty in describing the effect of nanoscale phase separation on the performance of organic photovoltaics (OPVs) illustrates the need for further examination of the role of mixing and transport within organic semiconductor mixtures [5-9]. Kozub et al. has recently shown that regioregular poly(3-hexylthiophene) (RR P3HT)/phenyl-C_{61}-butyric acid methyl ester (PCBM) mixtures, which are used as the active layer of OPVs, separate into two phases due to the crystallization of the polymer [10]. The RR P3HT-rich phase, composed of P3HT crystals, is essentially pure. The PCBM-rich phase, however, is a mixture of amorphous P3HT with PCBM. The existence of a mixed phase is consistent with the semicrystalline nature of RR P3HT and the partial miscibility of P3HT and PCBM [10-12]. Except for highly immiscible systems, polymer/small molecule mixtures will always exhibit partial miscibility and as a consequence, mixed phases [10, 13]. Nevertheless, the effect of mixed phases on the efficiency of OPVs is not

clear; for instance, blending of organic semiconductors can strongly affect charge transport in mixtures [2, 14-19] and as a result affect OPV device performance.

Studies of charge transport in mixtures of organic semiconductors have demonstrated that, in general, carrier mobilities depend monotonically on the concentration of the carrier phase [15, 20-23]. As might be expected, a decrease in concentration of the carrier phase decreases the effective mobility. Consequently, efficient ambipolar transport is only achieved for a limited range of concentrations, which is system-specific. Studies are complicated by the semicrystalline nature of many organic semiconductors, since crystallization of one or more of the constituents can affect the composition of the remaining mixed amorphous phase. It remains a challenge to fully describe charge transport and its dependence on composition within mixed semiconductor films utilized in OPVs.

In this Letter, we examine a model system for the amorphous PCBM-rich phase prevalent in devices composed of RR P3HT/PCBM mixtures. By mixing regiorandom P3HT (RRa P3HT), which is amorphous, with PCBM, we create thin films which exhibit no crystallinity of either component. Thus, by fabricating thin film transistors we have examined the electron transport properties of amorphous P3HT/PCBM mixtures. We find that charge transport properties are closely coupled to the miscibility of the two components. At compositions where the films are miscible, PCBM is dispersed in RRa P3HT and electron transport is strongly suppressed. In contrast, when the materials are immiscible, spinodal decomposition driven phase separation leads to efficient electron transport by promoting percolating pathways throughout the active layer. Thus, our results suggest that charge transport in mixed amorphous systems is strongly coupled to the miscibility of the components and when homogeneous, can be described with percolation theory.

The photoactive layer morphologies of 1:1 by mass RR P3HT/PCBM solar cells are shown in Figure 1. The images are generated through energy-filtered transmission electron microscopy (EFTEM), which couples spectroscopy and microscopy to map the local elemental composition. The fiber-like morphologies are a direct consequence of the crystallization of P3HT, where the matrix phase is fullerene-rich but contains significant amorphous P3HT [10]. From the image intensities of Figure 1, we compute that the P3HT fibers are essentially pure (ca. 99%), but the PCBM-rich phases contain 30±5% and 45±4% P3HT by volume once annealed at 165 and 190 ^{o}C, respectively (see reference [10] for details of the calculation). Thus, Figure 1 demonstrates that the composition of the fullerene-rich phase, which is responsible for electron transport in OPVs, can depend on the crystallization of the components and processing conditions. Figure 1 exemplifies one of the challenges in examining electron transport in semicrystalline polythiophene/fullerene mixtures; crystallization can affect the composition of the fullerene-rich phase. On the other hand, Figure 1 also suggests that electron transport is likely not a trivial function of electron donor/acceptor composition in OPVs.

As a model system for the matrix phase within the photoactive layer of RR P3HT/PCBM OPVs, we mix RRa P3HT, which does not crystallize, with PCBM at various compositions. The number-averaged molecular weight of RRa P3HT is 30 kg/mol (Sigma-Aldrich). RRa P3HT was extensively purified through precipitation in methanol and soxhlet extraction in hexane, hexane/methanol and methanol. Mixtures were created through dissolution in anhydrous chlorobenzene and spun cast into thin films. The resulting films are amorphous for the processing conditions chosen in this study.

Bottom-contact, bottom-gate field-effect transistors were fabricated to examine the electron mobility of amorphous RRa P3HT/PCBM mixtures. All devices were fabricated and

tested in an N_2 glovebox. In order to prevent selective wetting at the dielectric-semiconductor interface, the surface energy of the dielectric was carefully modified. Near Edge X-ray Absorption Fine Structure studies of P3HT/PCBM films have shown that selective wetting occurs on various substrates [24, 25]. The composition of P3HT/PCBM films at SiO_2 (surfaces surface energy=77.4 dyn/cm [25]) is 18% P3HT, while on octotrichlorosilane (OTS) (23.7 dyn/cm [25]) the composition is 74% P3HT. Thus, we do not expect significant selective wetting on hexamethyldisilazane (HMDS), which has a surface energy of 43 dyn/cm [26]. Linearly interpolating between the surface energy of SiO_2 and OTS would suggest a composition on HMDS of 54% P3HT, close to the composition of the casting solution (58%). As a consequence, RRa P3HT/PCBM transistors are ideally suited for the examination of electron transport in organic semiconductor mixtures and to obtain insights into the fullerene-rich phase of RR P3HT/PCBM OPVs.

Figure 2a shows transfer characteristics of RRa P3HT/PCBM field effect transistors at three different PCBM volume fractions. Devices exhibit both hole and electron transport characteristics with threshold voltages near 80 V. The hole mobilities of both neat RRa P3HT and PCBM are ~ 10^{-6} to 10^{-5} cm^2/Vs. Consequently, hole mobilities of mixed films do not vary significantly with composition. The electron mobilities (μ_e) at PCBM volume fractions (ϕ_{PCBM}) of 0.4, 0.55 and 0.7 are $2.5\pm0.3\times10^{-5}$, $2.2\pm0.1\times10^{-4}$, and $1.8\pm0.6\times10^{-3}$ cm^2/Vs, respectively; μ_e varies with composition and approaches the neat μ_e of PCBM, μ_e^0, with increasing ϕ_{PCBM} ($\mu_e^0=2.6\pm0.7\times10^{-3}$ cm^2/Vs from our studies and 10^{-3} to 10^{-2} cm^2/Vs in the literature [15, 20-23, 27, 28]). Figure 2b summarizes μ_e in the saturation regime calculated from transfer curves as a function of ϕ_{PCBM} for RRa P3HT/PCBM transistors. Mobilities were calculated at gate voltages which are 20-30 V above the threshold voltage resulting in charge densities near $1\text{-}2\times10^{12}$ cm^{-2}.

Devices were tested as cast or annealed at either 50 or 100 ^{o}C for 12 hrs. The time and temperature for thermal annealing was chosen to prevent PCBM crystallization [29]. Data from as-cast RR P3HT/PCBM transistors is also shown in Figure 2b, since RR P3HT/PCBM films which are not annealed exhibit little structure [10, 30]. For all of the processing conditions chosen for this study, μ_e does not depend on processing conditions. Furthermore, as shown in Figure 2c, μ_e depends linearly on composition when ϕ_{PCBM}>0.6. In contrast, μ_e decreases super-linearly as the amount of PCBM is decreased in the film for ϕ_{PCBM}<0.6 (Figure 2b). The sudden change in μ_e from a super-linear to linear dependence on composition has not been observed in previous studies of the mobility in RR P3HT/PCBM films, which possess significant P3HT crystallinity due to thermal annealing [15, 21]. By utilizing RRa P3HT and controlling the processing conditions, our studies uniquely examine electron transport in amorphous films.

Figure 3 shows μ_e as a function of temperature for ϕ_{PCBM}=0.8 and 0.4. The increase in mobility with increasing temperature is due to thermally activated transport, commonly observed in organic semiconductors [31]. Although μ_e varies by two orders of magnitude, the temperature dependence and consequently the activation energy, E_a, is unchanged. Furthermore, E_a from our blends (83 meV for ϕ_{PCBM}=0.8 and 73 meV for ϕ_{PCBM}=0.4) is similar to E_a from studies on PCBM films (63-100 meV) [27, 28, 32]. The similar E_a values from our blends and neat PCBM suggest that transport is occurring through PCBM molecules only; in addition, at ϕ_{PCBM}=0.8 it is unlikely that electron hopping is limited by RRa P3HT due to the high PCBM content. Thus, Figure 3 demonstrates that the dominant phenomena that leads to activated transport is unperturbed as a function of composition. This implies that intermolecular charge hopping, trap densities and the temperature dependence of percolating pathways do not change significantly with ϕ_{PCBM}. As a result, we assume that electron hopping takes place only through PCBM and

not through RRa P3HT and we attribute the drop in the room temperature mobility below ϕ_{PCBM}=0.6 to a decrease in the number of percolating pathways within the active layer.

Concepts from percolation theory are powerful in describing the electrical properties of composites [33-35]. In particular, the conductivity of a composite system is given by $(\phi-\phi_c)^{\alpha}$ near the percolation threshold, where ϕ_c is the percolation volume fraction and α is an exponent which depends on the dimensionality of the sample. We note that ϕ_c can depend on the intermolecular interactions within the system and has been observed to vary between 0.07 and 0.65 in various mixtures [34]. The electron mobility for our system at ϕ_{PCBM}=0.16 is 1.4×10^{-7} cm^2/Vs, but at ϕ_{PCBM}=0.14 the value is too low to measure with our instrumentation ($\mu_e<10^{-10}$ cm^2/Vs). Thus, we take ϕ_c to be 0.15±0.01. Figure 4 shows the electron mobility as a function of (ϕ_{PCBM}-ϕ_c). μ_e increases with (ϕ_{PCBM}-ϕ_c) until (ϕ_{PCBM}-ϕ_c)≈0.45, after which μ_e depends linearly on (ϕ_{PCBM}-ϕ_c).

The data in Figure 4 follow percolation behavior for small (ϕ_{PCBM}-ϕ_c); mobilities approaching the percolation threshold follow a scaling law for conductivity in 3D percolating systems (α=2) [33, 34]. Figure 4 denotes $\mu_e \propto (\phi_{PCBM}-\phi_c)^2$ as a solid line for comparison to the data. In addition, fitting the three data points with lowest (ϕ_{PCBM}-ϕ_c) yields α=2.2±0.2, where the error is computed by considering the range of ϕ_c (0.15±0.01). Our data is not consistent with a 2D exponent(α=1.3) [33, 35], suggesting that the channel region is sufficiently thick to allow multiple layers of fullerene to participate in conduction. A channel thickness of 3-5 nm is not unreasonable for organic semiconductors [36]; furthermore, field-effect mobilities in organic semiconductors saturate only after 3 or more layers are deposited [37, 38]. Nevertheless, we note that a high gate bias may decrease the channel thickness and effectively constrain charge transport to 2D conduction [39]. As (ϕ_{PCBM}-ϕ_c) approaches 0.45, μ_e no longer follows (ϕ_{PCBM}-

$\phi_c)^2$. Both the divergence of μ_e from the expected scaling law and the linear dependence of μ_e on composition after (ϕ_{PCBM}-ϕ_c)≈0.45 are not consistent with percolation theory. Thus, factors other than simple percolation of homogeneously dispersed PCBM molecules in a RRa P3HT matrix must play a role in governing electron transport for (ϕ_{PCBM}-ϕ_c)>0.45.

We have previously determined the miscibility of amorphous P3HT/PCBM mixtures [10]. By measuring the melting point depression of RR P3HT when mixed with PCBM, we were able to estimate the Flory-Huggins interaction parameter, χ, and the compositions for which the components are miscible. From Flory-Huggins theory, we found that for ϕ_{PCBM}>0.58±0.05 amorphous P3HT and PCBM are immiscible; this miscibility limit is denoted in Figure 4 as a gray region to include the experimental uncertainty. Once immiscible, the number of percolation pathways of the majority phase is enhanced by the formation of distinct phases. The Flory-Huggins phase diagram for amorphous P3HT/PCBM mixtures shown in Figure 3 of reference [10] predicts that once immiscible, a pure PCBM phase will form. Thus, we expect the mobility will decrease linearly with dilution from the neat PCBM electron mobility, μ_e^0. Although our data has significant scatter, we note that the average electron mobility of all samples increases linearly for (ϕ_{PCBM}-ϕ_c)>0.43 (or ϕ_{PCBM}>0.58, see Figure 2c). We speculate that the rapid increase near (ϕ_{PCBM}-ϕ_c)=0.4 of μ_e from (ϕ_{PCBM}-ϕ_c)^2 to a $\phi_{PCBM}\times\mu_e^0$ dependence is due to concentration fluctuations as immiscibility is approached. The linear dependence of the mobility with composition at (ϕ_{PCBM}-ϕ_c)>0.43 (Figures 2c and 4), however, is clearly due to the components becoming immiscible at this composition.

Energy-filtered transmission electron microscopy (EFTEM) was used to generate high contrast images of the morphologies in amorphous mixtures of RRa P3HT/PCBM. As shown in Figure 5a, at high ϕ_{PCBM} (ϕ_{PCBM}=0.8 and 0.7) light regions corresponding to P3HT-rich domains

and dark regions corresponding to PCBM-rich domains are visible. The presence of distinct P3HT and PCBM domains demonstrates that polythiophene/fullerene mixtures are not completely miscible. In contrast, the sulfur elemental map for ϕ_{PCBM}=0.2 shows no evidence of phase separation, indicating that RRa P3HT and PCBM are miscible. Figure 5b shows the radially-averaged fast Fourier transform (FFT) intensities as a function of the reciprocal space scattering vector, q, generated from the EFTEM images in Figure 5a. There is a jump in the FFT intensities between ϕ_{PCBM}=0.6 and 0.7 for $q < 0.28$ nm^{-1}, suggesting coarsening and growth of structures greater than 22 nm for samples with high PCBM compositions. This is illustrated by the change in slope in the integrated FFT intensities shown in the inset of Figure 5b. Thus, the results shown in Figures 5a and 5b are consistent with our previous measurements of the miscibility limit of P3HT/PCBM mixtures at ϕ_{PCBM}=0.58±0.05 [10] and support our hypothesis that the drop in the mobility when ϕ_{PCBM}<0.58 is due to RRa P3HT/PCBM mixtures becoming homogeneous.

Through a combination of our previous measurements of the miscibility [10], and the EFTEM results shown in Figure 5, we conclude that at high fullerene volume fractions PCBM and RRa P3HT are immiscible. Consequently, the components phase separate and μ_e is the product of the neat PCBM mobility and ϕ_{PCBM} (Figure 2c). Immiscibility of the two components promotes percolating pathways, thereby enhancing charge transport in the mixture. On the other hand, at low PCBM volume fractions, the components are miscible. As ϕ_{PCBM} decreases, the number of percolating pathways also decreases resulting in drastically lower mobilities. Consequently, we surmise that the extent of miscibility between donor and acceptor components in OPVs can affect device performance by governing charge transport within the photoactive layer. Donor/acceptor mixtures which are completely miscible would exhibit sharp drop offs in

charge transport efficacy with dilution. Strongly immiscible systems, on the other hand, would readily phase separate into large domains and prevent efficient charge separation. Our results suggest that partial miscibility of donor/acceptor mixtures is critical for efficient device performance.

In summary, we have demonstrated the interplay between miscibility and percolation in a model organic semiconductor mixture. We utilized field-effect mobilities derived from thin-film transistors as a measure of the conductive pathways present in amorphous polythiophene/fullerene blends. This approach examines electron transport in the fullerene-rich phase of polythiophene/fullerene solar cells and can be extended to crystalline polymer/fullerene mixtures if the compositions near the dielectric interface are known. Our study reveals that the electron mobility of amorphous mixtures of RRa P3HT/PCBM decreases significantly below fullerene volume fractions of 0.58, where the components are miscible. The strong dependence of charge transport on the miscibility of P3HT and PCBM suggests that partial miscibility may be critical for efficient OPV device performance.

Tom Jackson and Haouyu Li are gratefully acknowledged for assistance in fabricating thin-film transistors. Major funding for this work was provided by NSF under Award DMR-1056199. The authors also acknowledge support of the National Center for Electron Microscopy, Lawrence Berkeley National Laboratory, which is supported by the U.S. Department of Energy under Contract No. DE-AC02-05CH11231.

References and Notes

[1] M. M. Alam, and S. A. Jenekhe, Macromolecular Rapid Communications **27**, 2053 (2006).

[2] D. K. Hwang *et al.*, Advanced Materials **23**, 1293 (2011).

[3] S. E. Shaheen, D. S. Ginley, and G. E. Jabbour, MRS Bulletin **30**, 10 (2005).

[4] C. J. Brabec *et al.*, Advanced Materials **22**, 3839 (2010).

[5] B. C. Thompson, and J. M. J. Fréchet, Angewandte Chemie International Edition **47**, 58 (2008).

[6] X. Yang *et al.*, Nano Letters **5**, 579 (2005).

[7] Y. Liang *et al.*, Advanced Materials **22**, E135 (2010).

[8] C. Muller *et al.*, Advanced Materials **20**, 3510 (2008).

[9] C. R. McNeill *et al.*, Nano Letters **6**, 1202 (2006).

[10] D. R. Kozub *et al.*, Macromolecules **44**, 5722 (2011).

[11] B. A. Collins *et al.*, Journal of Physical Chemistry Letters **1**, 3160 (2010).

[12] N. D. Treat *et al.*, Advanced Energy Materials **1**, 82 (2011).

[13] S. Swaraj *et al.*, Nano Letters **10**, 2863 (2010).

[14] H. J. Snaith *et al.*, Nano Letters **2**, 1353 (2002).

[15] J. Y. Kim, and C. D. Frisbie, The Journal of Physical Chemistry C **112**, 17726 (2008).

[16] P. W. M. Blom *et al.*, Advanced Materials **19**, 1551 (2007).

[17] V. D. Mihailetchi *et al.*, Advanced Functional Materials **16**, 699 (2006).

[18] N. C. Cates *et al.*, Chemistry of Materials **22**, 3543 (2010).

[19] S. Goffri *et al.*, Nature Materials **5**, 950 (2006).

[20] M. Morana *et al.*, Advanced Functional Materials **17**, 3274 (2007).

[21] E. von Hauff, J. Parisi, and V. Dyakonov, Thin Solid Films **511-512**, 506 (2006).

[22] M. Morana *et al.*, Advanced Functional Materials **18**, 1757 (2008).

[23] J. Nakamura, K. Murata, and K. Takahashi, Applied Physics Letters **87**, 132105 (2005).

[24] H. Wang *et al.*, Chemistry of Materials **23**, 2020 (2011).

[25] D. S. Germack *et al.*, Applied Physics Letters **94**, 233303 (2009).

[26] S. C. Lim *et al.*, Synthetic Metals **148**, 75 (2005).

[27] M. Chikamatsu *et al.*, Chemistry of Materials **20**, 7365 (2008).

[28] M. Chikamatsu *et al.*, Applied Physics Letters **87**, 203504 (2005).

[29] A few small crystallites were observed with a light microscope for RRa P3HT/PCBM films annealed at 100 degrees for 12 hrs. For this set of data, only devices which contain no crystals within the channel region or in the sorrounding regions were tested.

[30] E. D. Gomez *et al.*, Chemical Communications **47**, 436 (2011).

[31] H. Sirringhaus, Advanced Materials **17**, 2411 (2005).

[32] T. B. Singh *et al.*, Journal of Applied Physics **97**, 083714 (2005).

[33] D. Stauffer, and A. Aharony, *Introduction to Percolation Theory* (Taylor and Francis, London, 1992).

[34] P. S. Clarke, J. W. Orton, and A. J. Guest, Physical Review B **18**, 1813 (1978).

[35] S. Kirkpatrick, Reviews of Modern Physics **45**, 574 (1973).

[36] C. Tanase *et al.*, physica status solidi (a) **201**, 1236 (2004).

[37] A. Shehu *et al.*, Physical Review Letters **104**, 246602 (2010).

[38] F. Dinelli *et al.*, Physical Review Letters **92**, 116802 (2004).

[39] N. Tessler *et al.*, Advanced Materials **21**, 2741 (2009).

Figure 1

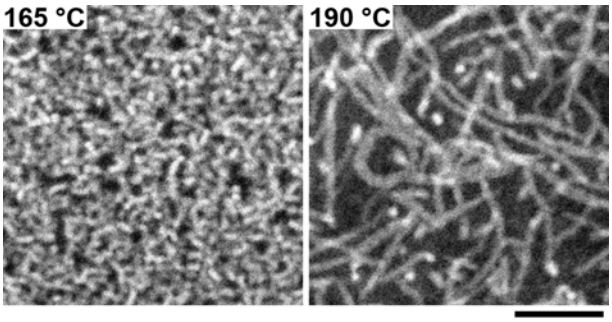

Sulfur elemental maps of 1:1 RR P3HT:PCBM mixtures (ϕ_{PCBM}=0.42) annealed at two different temperatures (165 and 190 ºC) generated through EFTEM. Samples were annealed for 30 min. The scale bar is 200 nm.

Figure 2

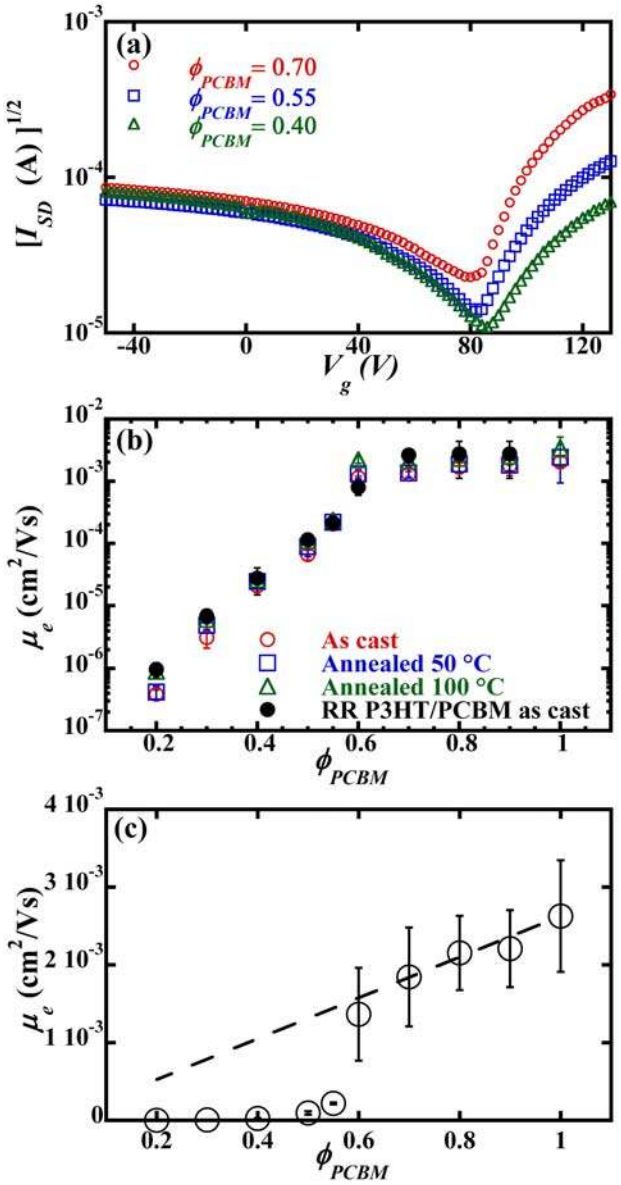

(Color online) (a) Transfer characteristics of RRa P3HT/PCBM field effect transistors at various PCBM volume fractions (channel widths of 220 μm and lengths of 20 μm). Samples were annealed at 50 ºC for 12 hours. (b) Electron mobility as a function of PCBM volume fraction for various processing conditions. Samples were annealed for 12 hrs. The electron mobility of as cast RR P3HT/PCBM devices is also shown. Error bars denote the standard deviation of multiple measurements. (c) μ_e averaged over all samples shown in (b) as a function of ϕ_{PCBM}. The errors bars denote the standard deviations. The dashed line is $\mu_e^0 \times \phi_{PCBM}$.

Figure 3

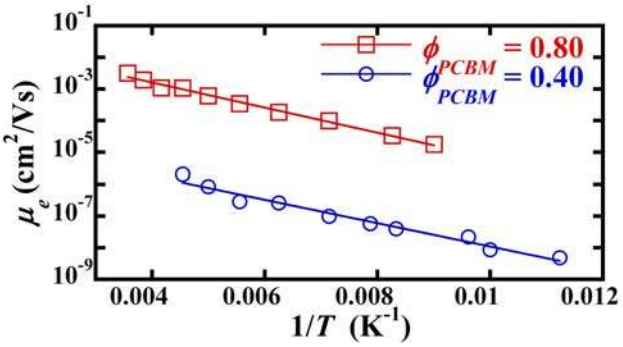

(Color online) Electron mobility as a function of temperature for ϕ_{PCBM}=0.8 and 0.4. The solid lines are exponential fits to the data.

Figure 4

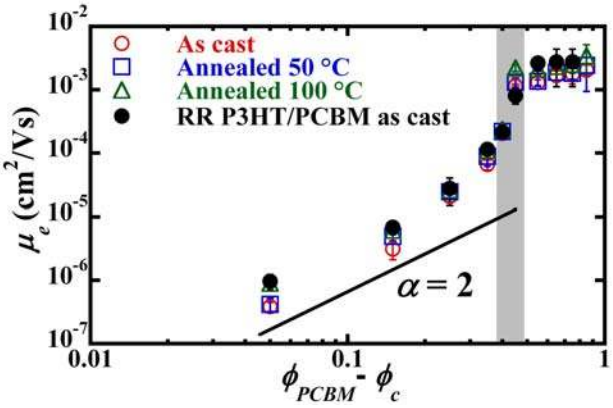

(Color online) Electron mobility of RRa P3HT/PCBM and RR P3HT/PCBM films for different processing conditions as a function of (ϕ_{PCBM}-ϕ_c). The solid line represents (ϕ_{PCBM}-ϕ_c)$^{\alpha}$ with a =2. The gray region designates the miscibility limit for P3HT/PCBM. Error bars denote the standard deviations of multiple measurements.

Figure 5

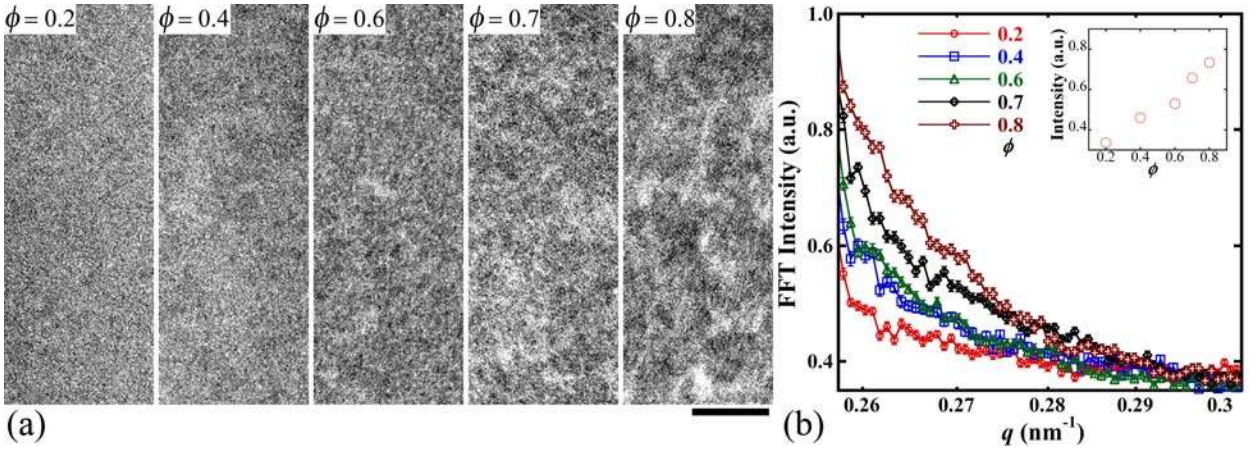

(Color online) (a) Sulfur elemental maps of RRa P3HT/PCBM mixtures at various PCBM volume fractions(ϕ=ϕ_{PCBM}). Samples were annealed at 50 ºC for 12 hours. The scale bar is 200 nm. (b) Fast Fourier transform (FFT) intensity as a function of scattering vector, q, obtained from the images in (a). Inset: FFT integrated intensity as a function of ϕ=ϕ_{PCBM}.